British Journal of Pharmacology (1995) 116, 3005-3013

Pentobarbitone modulation of NMDA receptors in neurones isolated from the rat olfactory brain

P. Charlesworth, *I. Jacobson & [1]C.D. Richards

Department of Physiology, Royal Free Hospital School of Medicine, Rowland Hill Street, London NW3 2PF and *Department of Anatomy and Cell Biology, University of Goteborg, Medicinaregatan 5, S 413 90, Goteborg, Sweden

1 The action of pentobarbitone on the N-methyl-D-aspartate (NMDA) receptors of neurones freshly dissociated from the olfactory bulb and olfactory tubercle has been studied using patch-clamp techniques.

2 Pentobarbitone produced a concentration-dependent depression of the currents evoked by NMDA with an IC_{50} value of c. 250 μM.

3 Analysis of the NMDA-evoked noise produced power spectra that could be fitted by the sum of two Lorentzians with corner frequencies of 17 and 82 Hz. Pentobarbitone increased the corner frequency of the high frequency component but did not alter the apparent single channel conductance estimated from the noise.

4 Single channel recordings in either the cell-attached or outside-out patch configurations revealed that NMDA (20 or 50 μM) opened channels with a main conductance level around 55 pS and a principal subconductance around 44 pS. The uncorrected mean open time of the channels was 3.4 ms and mean burst length was 6.0 ms. Mean cluster length was about 12 ms.

5 Pentobarbitone produced a concentration-dependent reduction in both mean open time and burst length. Mean cluster length was much less affected. Pentobarbitone did not decrease unitary current amplitude or bias the open-state current amplitude distribution in favour of a particular substate.

6 From these data it appears that pentobarbitone depresses the inward current evoked by NMDA by reducing the probability of channel opening and this results from a shortening of the lifetime of the channel open state and by decreasing burst length.

Keywords: Olfactory bulb; olfactory tubercle; NMDA receptor; patch clamp; noise analysis; single channels; pentobarbitone; barbiturate

Introduction

General anaesthetics are known to depress excitatory synaptic transmission but the underlying mechanisms remain incompletely resolved. There is evidence that anaesthetics depress both the secretion of transmitters and the response of post-synaptic receptors but determination of the precise mechanism of synaptic blockade requires detailed study of those synapses where the identity of the transmitter is reasonably certain. The acidic amino acid glutamate is widely considered to be a major excitatory transmitter at synapses within the CNS and there is good evidence to suggest that it acts in this role in the olfactory system (Sandberg *et al.*, 1984; Jacobson & Hamberger, 1986; Jacobson *et al.*, 1986). In addition, in the olfactory cortex it has been shown that general anaesthetics, including pentobarbitone, depress both excitatory synaptic transmission and the sensitivity of neurones to ionophoretically-applied glutamate (Richards *et al.*, 1975; Richards & Smaje, 1976). Similar results have been reported for the action of barbiturates on the glutamate sensitivity of neurones in the cat neocortex (Crawford & Curtis, 1966). Since these early studies it has become clear that glutamate acts on two major classes of receptor: ionotropic receptors which are integral parts of ion channels and metabotropic receptors which activate second messenger systems.

Ionotropic glutamate receptors are of two principal types which are named after their preferred agonists: NMDA (N-methyl-D-aspartate) and kainate/AMPA (α-amino 3-hydroxy-5-methyl isoxazole-4-propionic acid) (Watkins *et al.*, 1990). The kainate/AMPA receptor is currently considered to mediate fast excitatory synaptic transmission while the NMDA receptor has been implicated in synaptic plasticity (Headley & Grillner, 1990; Gasic & Heinemann, 1991). To date there have been few studies of the action of general anaesthetics on the sub-types of ionotropic receptor although barbiturates have been shown to depress the sensitivity of hippocampal neurones to ionophoretically-applied NMDA and kainate (Sawada & Yamamoto, 1985). Moreover, pentobarbitone has been found to block currents activated by kainate and L-aspartate more effectively at negative membrane potentials (Miljkovic & MacDonald, 1986). Unlike nictonic receptors which have relatively simple kinetics, NMDA receptors have multiple open and closed states (Gibb & Colquhoun, 1992). Openings occur in bursts and clusters and they have multiple conductance levels (Cull-Candy & Usowicz, 1989). The effects of anaesthetics on such intricate gating poses a number of interesting problems: Is it possible to describe the effects of an anaesthetic on NMDA receptors in terms of a simple kinetic model? Are some modes of gating more resistant to modulation by anaesthetics than others? Do anaesthetics change the balance between the different conductance levels? The work described in this paper set out to address these issues. A preliminary account of this work has been presented to the Physiological Society (Charlesworth *et al.*, 1994).

Methods

Cell preparation

Neurones were enzymatically dissociated from slices of olfactory bulb and olfactory tubercle obtained from 10-14 day old rats using protease from *Aspergillus oryzae* (olfactory bulb) or trypsin IX (olfactory tubercle) (Kay & Wong, 1986; Jacobson

[1] Author for correspondence.

& Li, 1992). All experiments on these cells were performed on small phase bright cells of less than 15 μm diameter. Judged by their morphology and their ability to generate voltage-activated inward and outward currents, these cells were interneurones.

Electrophysiological methods

Experiments were carried out using three variants of the patch-clamp recording technique of Hamill *et al.* (1981). The configurations used were on-cell (cell attached) recording, whole cell recording under voltage clamp and recording from excised outside-out patches. It was necessary to use cultured neurones for excised patches owing to the stronger attachment of these cells to the substrate. Hippocampal neurones grown for 4–7 days in culture provided a reliable source of culture material. Patch pipettes were fabricated from thick-walled borosilicate glass (Clarke Electromedical GC150) and had tip diameters of 1–2 μm. The electrode tips were fire polished on a microforge prior to use. Their resistance was 5–15 MΩ and the series resistance was usually less than 20 MΩ. As the input resistance of the cells was more than 1 GΩ in all of our recordings and as the currents flowing through the pipette during the experiment were small, the voltage errors due to series resistance were also small and membrane holding potentials were not corrected for these errors. All experiments were performed at room temperature, 18–22°C.

Recording and analysis

Signals were recorded with either a List electronic L/M EPC-7 or Axopatch 1D patch clamp amplifier and were stored on magnetic tape (flat bandwidth DC-10 or DC-20 kHz). For analysis of whole cell current noise the signal from the tape recorder was filtered with a 8-pole Butterworth filter (bandpass DC-1 kHz) and digitised at 2.1 kHz. Records were divided into 0.4 s blocks prior to calculation of the spectral density (see Cull-Candy *et al.* (1988) for further details). N-methyl-D-aspartate was applied for at least 30 s in order to acquire sufficient time blocks for averaging of the spectra. Each spectrum was derived from a single continuous application. The mean power spectrum was calculated by averaging at least thirty of the spectra obtained from the 0.4 s time blocks. To obtain the noise spectrum due to application of agonist, the spectrum obtained prior to application of agonist was subtracted from that obtained during its application. The resulting spectra were then fitted by either a single or a double Lorentzian function using a least-squares Levenberg-Marquardt algorithm with proportional weighting of the data points. The quality of the fitted curve was judged from the value of χ^2 and the random distribution of residuals. The amplitude of single channel currents was estimated from the parameters derived from the fitted power spectra and the mean inward current (see Cull-Candy *et al.*, 1988). The spectral noise anlaysis (SPAN) was kindly supplied by Dr John Dempster, University of Strathclyde, U.K.

The single channel current derived from the noise spectra was calculated from the relation:

$$\gamma_{app} = \frac{S^2}{(E - E_r)\, I_m (1 - P_o)}$$

where S^2 is the variance of the noise, I_m the mean current, E the holding potential and E_r the reversal potential for the current (here taken as 0 mV) and P_o the probability of channel opening, which was assumed to be small because the current and associated noise was measured after the initial phase of desensitization (e.g. see Figure 1) and the concentration of agonist used was less than a fifth of that required for a maximal response.

Single channel records were obtained using cell attached or outside-out patches. For cell attached patches, the patch pipette contained NMDA (50 μM) in Mg^{2+}-free Locke solution containing 5 μM glycine together with an appropriate concentration of pentobarbitone (0 to 800 μM). With outside-out patches, the patch pipette was perfused with Mg^{2+}-free Na Locke or Mg^{2+}-free Na Locke containing NMDA (20 μM) and glycine (5 μM) with pentobarbitone (400 μM). Records of single channel activity were obtained during continuous application of agonist.

For single channel analysis, stretches of records 30 to 400 s in length were filtered at 3 or 5 kHz with a six pole Bessel filter, digitized at 20 kHz or 25 kHz and analysed off-line using a CED 1401 interface and 386 computer. Each peak in the histogram of the distributions of current amplitudes was fitted by a Gaussian distribution function using the Levenberg-Marquardt, non linear, least squares method. In some experiments, the mean current values of the peaks at different patch potentials were subsequently used to construct the current-voltage relationship. The conductance of the channel was determined from the slope of the line of the current-voltage relationship. The channel dwell time histograms were constructed from lists of channel states by use of the transition detection method (Sachs *et al.*, 1982), the threshold for state transition being set at 50%. All double openings were rejected and data from those patches where more than 1% of openings were double openings were not included. The minimal resolvable event was about 100 μs and exponential fits to the histograms excluded the first histogram bin. Analysis software was kindly provided by Dr J. Dempster, University of Strathclyde.

Solutions

The external bathing medium (Locke solution) contained (mM) NaCl 140, KCl 5, $MgCl_2$ 1.8, $CaCl_2$ 1.0, HEPES 15, glucose 10; pH was adjusted to 7.4 with NaOH. For the experiments on NMDA the $MgCl_2$ was omitted and glycine (5–20 μM) was added. The pipettes used for whole cell recordings contained (mM) potassium methyl sulphate 120, Na methyl sulphate 20, $MgCl_2$ 2, $CaCl_2$ 1, EGTA 11 or KF 120, $MgCl_2$ 1, $CaCl_2$ 1, EGTA 11, HEPES 10; pH was adjusted to 7.2 with KOH and free calcium was measured as less than 10^{-7}M by use of an Orion 93-20 calcium electrode. Standard Locke solution containing 0.5 μM tetrodotoxin was used for recording from cell-attached patches and for excised outside-out patches 140 mM $CsMeSO_3$ was substituted for KCl and NaCl was omitted, the other ions were as for the whole cell recordings.

The glutamate agonists were applied by microperfusion using either a parallel arrangement of fused silica capilaries or a U-tube similar to that described by Krishtal & Pidoplichko (1980). Standard chemicals and the enzymes for tissue dissociation were obtained from Sigma Chemical Co and the NMDA from Tocris Neuramin (Bristol UK).

Statistical analysis

Combined values are shown as mean ± s.e.mean unless otherwise indicated. Differences between data sets were assessed by use of analysis of variance and were considered statistically significant when $P < 0.05$.

Results

The effects of pentobarbitone on whole cell currents evoked by NMDA

Characteristics of whole cell currents evoked by NMDA In all, more than 50 successful whole-cell recordings were made. At negative holding potentials, application of NMDA (10–500 μM) elicited a marked response in normal saline solution provided a Mg-free bathing medium containing glycine (5–20 μM) was used (see also Jacobson & Li, 1992). At positive holding potentials NMDA elicited a response even in the presence of Mg^{2+} provided that glycine was present in the

bathing solution. For the remaining experiments Mg-free solutions containing glycine were employed routinely (see experimental procedures) and the holding potential was set to −70 mV. Application of 200 μM NMDA elicited a marked inward current (mean 100±20 pA) which desensitized rapidly to a steady value (see Figure 1). This inward current had a reversal potential close to zero mV and was associated with an increase in noise (Figure 1).

The action of pentobarbitone on agonist-evoked currents For this study we have largely confined our attention to concentrations of pentobarbitone that lie within the anaesthetic range. Under the experimental conditions we have employed, application of pentobarbitone alone (25–400 μM) had no effect on the majority of cells. In 3/25 cells, however, application of pentobarbitone (>200 μM) evoked an inward current that had the characteristics of a $GABA_A$ current. These cells were excluded from the analysis presented here. Co-application of pentobarbitone with NMDA reduced the amplitude of the steady-state inward current in a concentration-dependent manner. Figure 2 shows the concentration-response relationship for the depressant effect of pentobarbitone on the steady-state response to 200 μM NMDA. The IC_{50} value for the action of pentobarbitone was about 250 μM. At concentrations between 25–400 μM the anaesthetic reduced both the peak current and steady-state current evoked by application of 200 μM NMDA by a similar amount (Figure 1). For example, the ratio of the steady-state current to peak current was 0.21±0.02 (n=12) in control and 0.19±0.05 (n=3) in 200 μM and 0.22±0.04 (n=6) in 400 μM pentobarbitone. The rate of current decline could be adequately fitted by a single exponential with a time constant of 0.64±0.10 s (n=10) in control, a value similar to that reported for isolated hippocampal neurones (Chizmakov *et al.*, 1992). As Figure 1 shows, pentobarbitone accelerated the rate of current decline. This effect was concentration-related and the time constant in 400 μM pentobarbitone was 0.28±0.02 s (n=5). In one cell (of six tested) the depressant effects of pentobarbitone increased progressively at negative holding potentials (−30 to −70 mV). In the remaining cells its effect was not obviously voltage-dependent (see Figure 1, lower panel). Pentobarbitone did not alter the reversal potential.

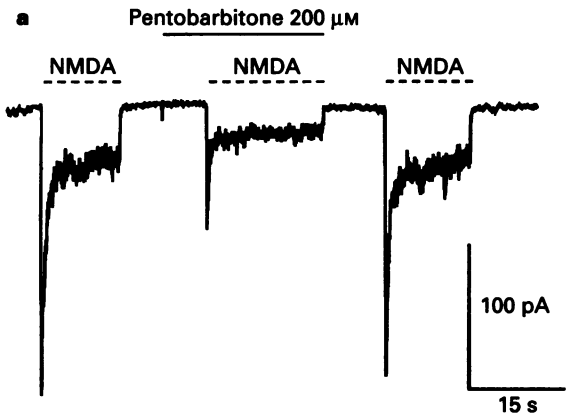

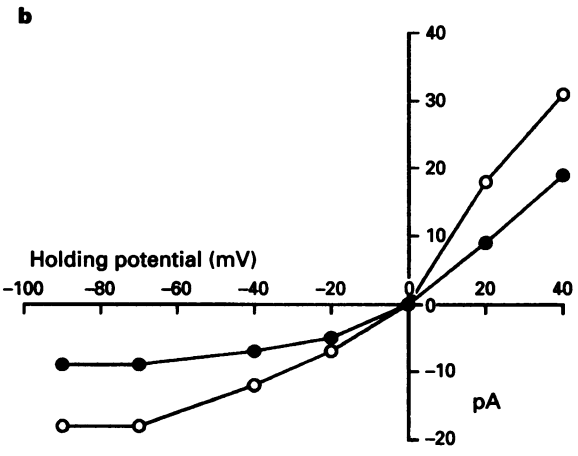

Figure 1 The effect of pentobarbitone on the inward current evoked by 200 μM N-methyl-D-aspartate (NMDA). (a) Shows a continuous stretch of record illustrating the reversible inhibition the whole cell current evoked by application of NMDA 200 μM by pentobarbitone 200 μM. The dotted lines show the periods during which NMDA was applied (holding potential −70 mV). Note that both peak and steady-state currents were reversibly depressed. (b) Shows the effect of pentobarbitone 200 μM (●) on the current-voltage relationship for NMDA-evoked currents over the range −90 to +40 mV. (○) Control.

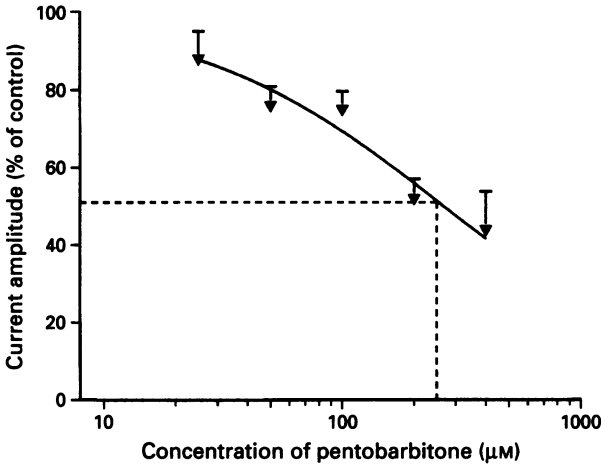

Figure 2 The concentration-response relationship for the action of pentobarbitone on steady-state currents evoked by application of N-methyl-D-aspartate (NMDA) 200 μM. The data are plotted±s.d. (n=4–7) and were fitted to a simple Langmuir adsorption isotherm (solid line). The IC_{50} value estimated from the concentration-response relation was about 250 μM.

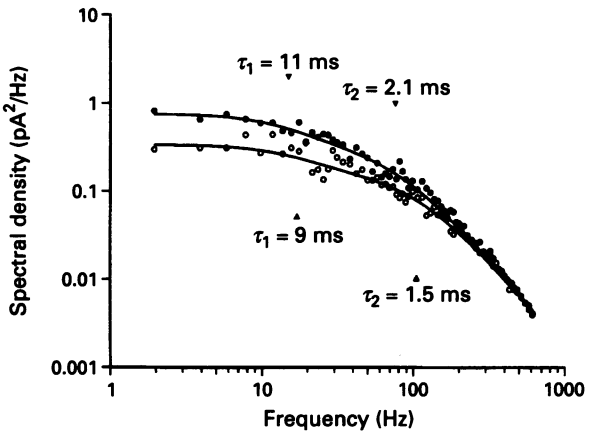

Figure 3 A typical example of the action of pentobarbitone on the power spectra of noise evoked by application of N-methyl-D-aspartate (NMDA). As the figure shows, power spectra derived from NMDA-evoked noise can be adequately fitted by the sum of two Lorentzians. (Their time constants are given by τ_1 and τ_2). Application of pentobarbitone 200 μM (○) did not induce any detectable extra component in the power spectrum but significantly reduced the time constant and decreased the zero frequency intercept of the fast component. (The corner frequency of the fast component increased from 76 Hz to 106 Hz). (●) Control.

Noise analysis As previously reported by Ascher *et al.* (1988), Cull-Candy *et al.* (1988) and Cull-Candy & Usowicz (1989), application of NMDA and other glutamate agonists is accompanied by an increase in signal noise. The plots of noise variance against mean current were linear (not shown) suggesting that the open probability was low and the single channel conductance estimated from the variance of the current noise was 45±3 pS and it was not altered by co-application of the anaesthetic (100–400 μM).

In general, when the noise evoked by NMDA (50–200 μM) was subjected to Fourier analysis, the resulting power spectra could be adequately fitted by the sum of two Lorenzians. The corner frequencies did not appear to depend upon the concentration of agonist applied. For 200 μM NMDA the spectra were well fitted by the sum of two Lorenzians with corner frequencies of 17±2.4 Hz and 82±7 Hz. The ratio of the zero frequency intercepts ($S(0)_1/S(0)_2$) was 2.4±0.6 (Figure 3 and Table 1). For a simple three state model of channel gating (see Ruff, 1977) these corner frequencies correspond to time constants in the region of 9.4 and 1.9 ms respectively. While the corner frequency of the slow component was not significantly altered by application of pentobarbitone that of the second (high frequency) component was increased (see Table 1). The zero frequency intercepts progressively decreased in amplitude with increasing concentrations of the anaesthetic. Nevertheless, the $S(0)_1/S(0)_2$ ratio changed very little suggesting that pentobarbitone did not have a selective effect on either component (see Figure 3 and Table 1).

Table 1 The spectral characteristics of N-methyl-D-aspartate (NMDA)-induced noise and its modification by pentobarbitone

Condition	F_{C1} (Hz)	F_{C2} (Hz)	$S(0)_1$ (pA^2)	$S(0)_2$ (pA^2)	$S(0)_1/S(0)_2$	γ (pS)	n
NMDA (0.2 mM)	17±2.4	82±7	0.78±0.09	0.41±0.06	2.4±0.60	45±3	8
NMDA (0.2 mM)+PB (0.1 mM)	15.0±3.1	117±11*	0.47±0.21	0.16±0.03	2.6±0.63	42±5	5
NMDA (0.2 mM)+PB (0.2 mM)	19±2.8	132±11*	0.42±0.14*	0.11±0.03	2.7±0.42	42±4	8
NMDA (0.2 mM)+PB (0.4 mM)	23±8	130±25*	0.26±0.12*	0.14±0.05	1.8±0.45	47±4	4

Key to abbreviations: F_{C1}, F_{C2} corner frequencies of the Lorenzian functions with zero frequency intercepts $S(0)_1$ and $S(0)_2$; PB: pentobarbitone. $S(0)_1/S(0)_2$ is the ratio of the zero intercepts. γ is the single channel conductance estimated from the noise spectra and mean current. *n* is the number of recordings. Statistical analysis of the data for pentobarbitone was always paired with respect to the relevant control data. All values are given as mean±s.e.mean. *Value significantly different to paired control value ($P<0.05$).

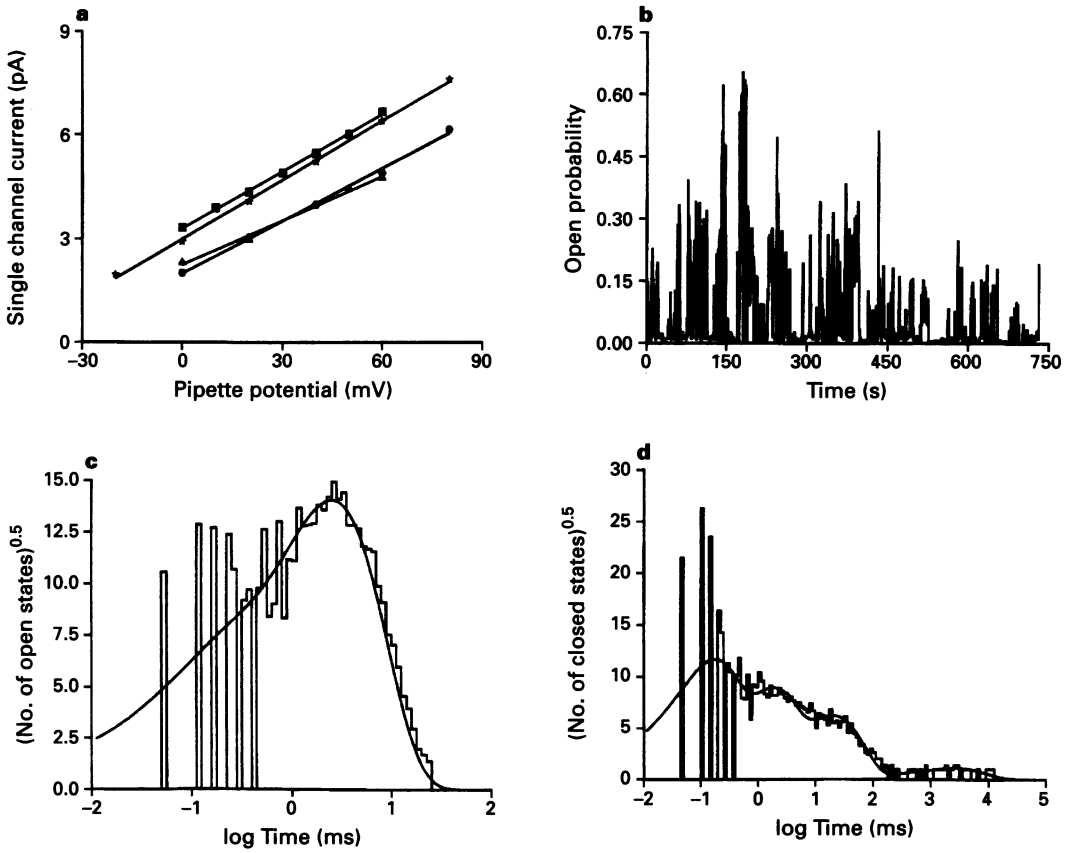

Figure 4 The effects of pentobarbitone on the properties of single N-methyl-D-aspartate (NMDA) channels. (a) The current-voltage relationship for single NMDA currents recorded from cell-attached patches of olfactory tubercle cells. The data are from two patches. Channels were activated by NMDA (50 μM) in the presence or absence of pentobarbitone (400 μM). The slope conductances are 55 and 42 pS for the full and subconductance levels in control (★, ●) and 57 and 51 pS in pentobarbitone (■, ▲). (b) Stability plot showing the open probability (P_o) of NMDA channel activity in 1 s epochs. Note the wide variation in P_o over the recording period. (c and d) The frequency distribution of NMDA channel open state and closed state dwell times. The ordinate gives the square root of the number of events and the abscissa scale is log dwell time (ms). The open times are fitted to the sum of two exponentials ($P_1 \exp(t/\tau_1)+P_2 \exp(t/\tau_2)$) where P_1 and P_2 represent the proportion of each component (0.097 and 0.90 respectively) and τ_1 and τ_2 are the time constants (0.16 and 2.52 ms respectively). The closed times are fitted to the sum of four exponentials where P_1 to P_4 are 0.39, 0.27, 0.28 and 0.065 and τ_1 to τ_4 are 0.16, 2.0, 50 and 1670 ms.

Single channel recording

Characteristics of NMDA channel openings in the absence of pentobarbitone Successful single channel recordings were obtained from more than 40 cell-attached patches. The maximum conductance level of the channel estimated from the slope of the voltage-current curve was around 55 pS (see Figure 4a). A second conductance level of about 44 pS was also observed and accounted for approximately 10% of open channel current. The threshold for detection of channel transitions was set to include both 44 pS and 55 pS openings. Under the recording conditions described in the Methods, the open probability (P_o) of the channels was generally low (with an average value of about 0.06) but it varied considerably over the recording time within a given patch. Periods during which the probability of opening was low were interspersed with brief periods of high P_o. Indeed P_o could vary more than ten fold between successive 1 s epochs within a given patch (see Figure 4b) (see also Gibb & Colquhoun, 1992).

The distribution of open states could be satisfactorily fitted to two exponentials with average time constants of 0.16 ms and 3.9 ms (see Figure 4c and Table 2). The ratio of the areas of the fast and slow components (A_f/A_s) was 0.27. The arithmetic mean open time was 3.4 ms. Closed times were best fitted by the sum of four exponentials with time constants of about 0.2, 2.0, 50 ms and 1700 ms (see Figure 4d and Table 2).

Following the convention adopted by Gibb & Colquhoun (1992) we have defined bursts and clusters of openings. Bursts were defined as closure less than a critical time (t_c) calculated from the closed time distributions for the first two components of each patch as described by Clapham & Neher (1984). The value of t_c was close to 0.4 ms (see Table 2). Mean burst length was near 6 ms and burst distribution could be adequately fitted by the sum of two exponentials with time constants of 0.10 and 6.75 ms (see Table 2). The areas of the fast and slow components were approximately equal ($A_f/A_s = 0.53$).

The value of t_c for clusters of channel openings was calculated in the same way as that for bursts but using the second and third components of the closed time distributions. The mean value of t_c was 4.57 ms. Mean cluster length was close to 12 ms and the clusters could be fitted by the sum of two exponentials with time constants of 0.22 ms and 13.6 ms (Table 2). The mean value of the ratio of the two components (A_f/A_s) was 0.28. For both bursts and clusters, the fast time constant (c. 0.1–0.2 ms) must represent single openings separated from true bursts or clusters (i.e. groups of openings) by an interval greater than t_c. Such isolated openings were rare.

Effects of pentobarbitone on the kinetics of NMDA channels When pentobarbitone was present in the pipette together with NMDA the mean channel open time was reduced in a concentration-dependent manner (Figures 5, 6 and Table 2) but there was no change in the amplitude of the unitary currents. The proportion of the 44 pS conductance level remained

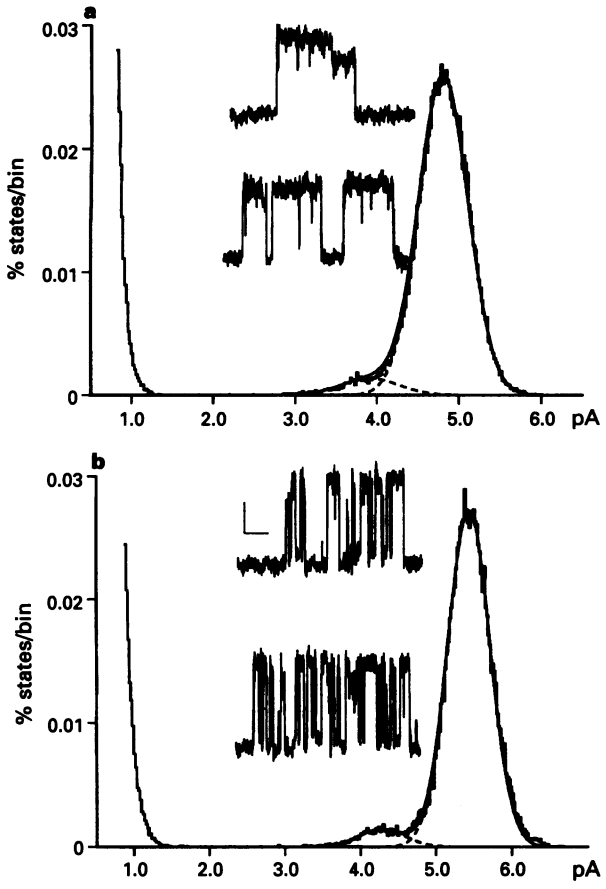

Figure 5 Single channel current amplitude distributions from two cell-attached patches. Note the minor contribution of the 80% subconductance state relative to the maximum conductance level. For clarity the data were processed by the running average procedure of Patlak (1988). The resulting distributions were fitted to the sum of two Gaussian curves. (a) Control distribution with two 80 ms sections of original record to show examples of the transitions. (b) Distribution of current amplitude in the presence of pentobarbitone 400 μM. The current traces show the typical brief closures induced by the drug. Horizontal scale bar 10 ms, vertical scale bar 2 pA.

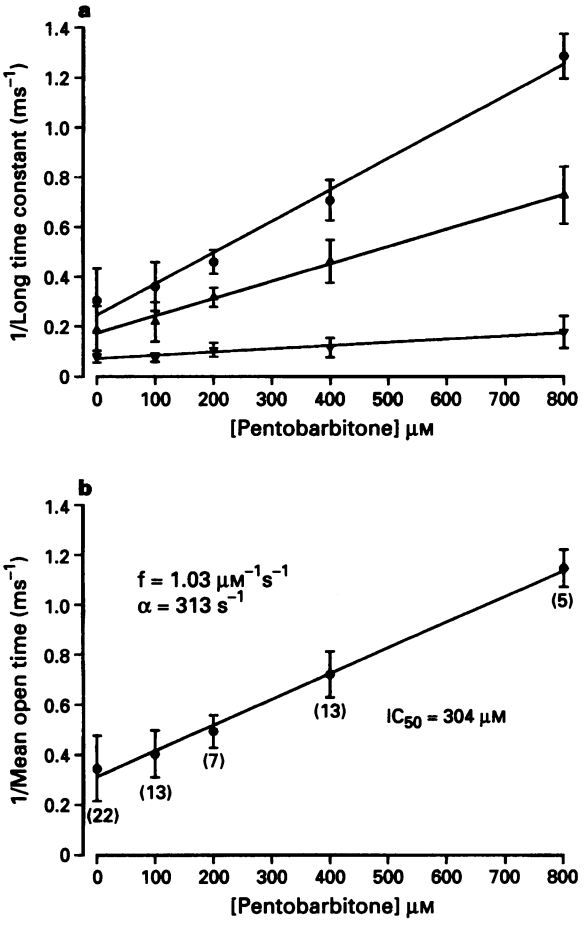

Figure 6 (a) The reciprocal of the long time constant from exponential fits of open (●), burst (▲) and cluster (▼) dwell time distributions plotted as a function of pentobarbitone concentration. (b) The reciprocal of mean open time plotted as a function of pentobarbitone concentration. The slope gives the rate constant for open channel block (f) and the intercept the aggregate rate constant for channel closure ($\alpha_1 + \alpha_2$) see Discussion. Error bars represent s.d. values and the *n* values are given in parentheses.

at 12%; other subconductance levels were not evident (see Figure 5). Furthermore, the single channel current amplitude distribution showed no peak corresponding to the predominant 29 pS conductance of $GABA_A$ Cl^- channels thus providing evidence that pentobarbitone did not activate these channels under the conditions employed in this study. As the P_o of the channels varied with time within a given patch, it was difficult to determine the concentration-response relationship for the effects of pentobarbitone on P_o. Nevertheless, P_o tended to decline with increasing concentrations of pentobarbitone. Thus in control P_o was $6.3 \pm 6.1\%$ ($n=17$), in 100 μM pentobarbitone it was $3.5 \pm 3.3\%$ ($n=8$) and in 800 μM it was $2.1 \pm 2.1\%$ ($n=3$).

Consistent with the fall in mean open time, the open time distributions revealed a progressive decline in the time constants for channel closure with increased pentobarbitone concentration. In addition, the distribution of open time was increasingly biased towards the first component. At the highest concentration of pentobarbitone, the distribution of the open times could be adequately fitted by a single exponential (Table 2).

The closed time distributions showed no statistically significant shift in the time constants of the second, third and fourth components but the time constant of the fastest component progressively increased with increased pentobarbitone concentration (Table 2). The area of the first and third components declined while that of the second component increased with increasing concentrations of pentobarbitone. (These effects were statistically significant by analysis of variance).

The mean burst length decreased in a concentration-related manner from near 6 ms in control to 1.3 ms in 800 μM pentobarbitone (Figure 6 and Table 2). The critical time for definition of a burst (t_c) showed no significant trend with increasing concentration of the anaesthetic. Examination of the distribution of burst length showed that the fast time constant altered very little with increasing pentobarbitone concentration but the slower time constant fell from 6.75 ms in control to 1.4 ms when 800 μM pentobarbitone was present in the patch pipette (Table 2). In addition, the distribution became biased towards the slower time constant. The number of brief closures within a burst (gaps) tended to fall with increasing concentrations of pentobarbitone but this effect was not statistically significant. Mean blocked time (the mean duration of the closures within a burst) did not alter.

The mean duration of clusters of channel openings also fell as the concentration of pentobarbitone increased but the decline was less marked than the decline in either mean open time or mean burst length. Thus, in control, mean cluster length was close to 12 ms but when 800 μM pentobarbitone was present in the patch pipette (the highest concentration tested) it fell to about 5.4 ms (Table 2 and Figure 6). The critical time for distinguishing clusters from bursts and the number of closures within a cluster (which must include the gaps within a burst) showed no systematic trend with increasing anaesthetic concentration. There was a clear tendency for the time constant of the second component of the cluster distribution to fall with increasing pentobarbitone concentration but the proportion of the fast and slow components did not change.

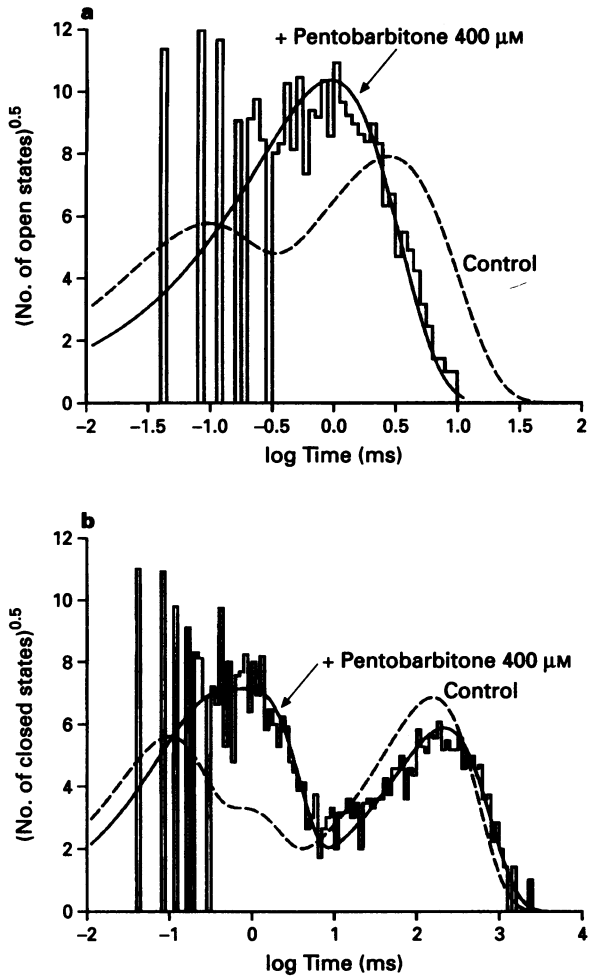

Figure 7 Dwell time frequency histograms for the action of pentobarbitone on single channel events recorded from an outside-out patch excised from a cultured hippocampal neurone. Channel openings were elicited by application of a stream of Locke solution containing N-methyl-D-aspartate (NMDA) 20 μM or NMDA (20 μM) and pentobarbitone (400 μM). Data bars and solid curve fits relate to data obtained during co-application of anaesthetic plus agonist, dashed lines are the curve fits to the paired control histograms. (a) Open state dwell time histogram data are fitted to the sum of two exponentials (control) or to a single exponential (pentobarbitone 400 μM). The time constants were τ_1 0.08 ms and τ_2 2.8 ms in control and τ was 0.95 ms in the presence of pentobarbitone 400 μM. (b) Closed state dwell time histogram. The data are fitted to the sum of three exponentials with time constants of 0.09, 0.78 and 157 ms in control (P_1 0.31, P_2 0.12 and P_3 0.55). In the presence of pentobarbitone 400 μM the time constants were 0.2, 1.2 and 215 ms (P_1 0.22, P_2 0.46 and P_3 0.33). Note that pentobarbitone shifts the distribution of the long closures to the right indicating fewer openings per unit time and increases the number of short closures.

The effect of pentobarbitone on excised outside-out patches In two excised outside-out patches the channel activity was sufficiently stable to permit recording of NMDA-activated channel activity before, during and after application of pentobarbitone. In the most stable of these recordings, pentobarbitone (400 μM) reduced the P_o of the channel from 2.4% to 1.4%. After washout of the anaesthetic P_o was higher than in control at 4.8%. In this patch mean open time in control was 2.3 ms ($n=1857$) falling to 1.0 ms ($n=2429$) when pentobarbitone was applied (Figure 7a). During washout of the drug the mean open time had risen to 5.1 ms ($n=274$) before the patch was lost. (The number of openings for each condition is given in parentheses). Burst length fell from 3.3 ms ($n=1306$) to 1.2 ($n=2010$) recovering to 7.8 ms ($n=184$) before the patch was lost. The t_c values were 0.29, 0.20 and 0.4 ms. Examination of the closed time distributions showed that there was an increase in the number of brief closures (see Figure 7b). In the second patch mean open times were 2.5 ms in control ($n=329$) and 1.1 ms ($n=394$) during application of pentobarbitone. In this case the patch was lost before full recovery occurred. Burst length was 4.0 ms ($n=215$) in control and 1.4 ms ($n=323$) in the presence of 400 μM pentobarbitone. These data are broadly in accord with the data from the cell-attached patches discussed above. In contrast, cluster length showed no consistent trend. (For patch 1 cluster length was 4.0 ms ($n=1117$) in control and 4.5 ms ($n=825$) in the presence of 400 μM pentobarbitone. For patch 2 the values were 5.1 ms ($n=182$) and 4.7 ms ($n=132$) respectively).

Table 2 Effect of pentobarbitone on (N-methyl-D-aspartate) (NMDA) channel kinetics (cell-attached patches)

		Pentobarbitone			
	Control	100 μM	200 μM	400 μM	800 μM
Open times					
τ_1	0.16±0.04	0.13±0.06	0.08±0.04*	0.07±0.05**	–
τ_2	3.9±1.7	2.9±0.7	2.2±0.23	1.4±0.17**	0.78±0.06**
Mean open time	3.4±1.4	2.6±0.48	2.1±0.27	1.4±0.17**	0.87±0.06**
Closed times					
τ_1	0.21±0.09	0.22±0.075	0.33±0.05	0.35±0.14**	0.54±0.17**
τ_2	1.9±0.75	1.70±0.49	1.7±0.49	1.4±0.36	1.5±0.38
τ_3	50±31	98±72	72±36	45±26	95±68
τ_4	1700±1400	3100±1800	2300±2100	1100±1100	950±430
Bursts					
t_c	0.41±0.07	0.39±0.16	0.42±0.12	0.43±0.20	0.58±0.25
τ_1	0.10±0.04	0.19±0.06	0.14±0.04	0.18±0.07	0.23±0.12
τ_2	6.8±2.9	5.2±2.2	3.20±0.40*	2.3±0.43**	1.4±0.22**
Mean burst length	6.0±2.8	4.6±2.0	2.9±0.4	2.2±0.4**	1.3±0.16**
Gaps/burst	0.67±0.31	0.68±0.40	0.39±0.14	0.46±0.19	0.38±0.14
Mean block time	0.18±0.03	0.17±0.05	0.20±0.04	0.20±0.08	0.27±0.10*
Clusters					
t_c	4.6±1.9	5.8±1.5	5.4±1.6	4.4±0.88	5.3±1.14
τ_1	0.22±0.12	0.25±0.12	0.17±0.07	0.27±0.24	0.27±0.15
τ_2	14±3.7	14±2.6	10±3.2	9.6±2.9*	6.7±2.8*
Mean cluster length	12±3.6	12.0±3.5	9.1±2.9	7.8±2.8*	5.4±2.50*
Gaps/cluster	2.1±0.85	2.8±0.90	2.2±0.82	2.7±1.1	2.1±0.81
Mean block time	0.80±0.37	0.89±0.22	1.1±0.22	0.96±0.16	1.2±0.3
No. of patches	17	8	3	9	3

All values in ms (mean±s.d.): τ_1, τ_2 etc are time constants in ms; t_c, critical time. *$P<0.05$, **$P<0.01$ by analysis of variance.

Discussion

The characteristics of the currents and of the noise evoked by application of NMDA agree well with previous descriptions (see Ascher *et al.*, 1988; Cull-Candy *et al.*, 1988; Cull-Candy & Usowicz, 1989; Jacobson & Li, 1992). The agonist-induced noise could be fitted by the sum of two Lorenzians with time constants of about 2 and 10 ms and the single channel conductance estimated from the variance of NMDA-evoked noise (γ_{noise}) was 45 pS. For comparison, Cull-Candy *et al.* (1988) obtained time constants of 1.5 and 7 ms and γ_{noise} 46.7 pS for two component spectra. Single channel analysis showed that the principal single channel conductance level was around 55 pS with a major subconductance level of about 44 pS, close to the values previously found by Cull-Candy *et al.* (1988) for cerebellar granule cells. The uncorrected mean open time was 3.4 ms in cell attached patches, burst length was 6 ms and cluster length (see Gibb & Colquhoun, 1992) was 12 ms. In excised outside-out patches the values were somewhat shorter: mean open time was about 2.5 ms, burst length about 3.5 ms and cluster length was about 5 ms. The differences between the data for cell-attached patches and excised patches may reflect the differing origins of the source material (dissociated cells vs cell culture) or the loss of some intracellular modulator during formation of the excised patches. Further work will be needed to clarify this point.

In agreement with the work of Sawada & Yamamoto, (1985) our data show that pentobarbitone inhibited the inward current evoked by NMDA and that this effect occurred at concentrations of pentobarbitone that lie within the anaesthetic range which is 50–300 μM (see Richards, 1972). The depression of inward current was not associated with any consistent change in the current-voltage relationship but pentobarbitone appeared to increase the rate at which the NMDA receptors desensitize. The failure of other groups to find similar sensitivity is difficult to explain (see Cai & McCaslin, 1993; Marszalec & Narahashi, 1993). It has been shown, however, that heteromeric recombinant NMDA receptors assembled from different subunits have distinct pharmacological properties (Kutsuwada *et al.*, 1992; Monyer *et al.*, 1992). Moreover, the expression of NMDA receptors changes during development (Williams *et al.*, 1993). The subunit composition of the native NMDA receptors studied here remains to be elucidated.

The principal object of the current series of experiments was to establish the mechanism by which pentobarbitone depresses the inward current evoked by application of NMDA. Analysis of the noise evoked by application of NMDA showed that pentobarbitone (100–400 μM) decreased the fast time constant although it did not alter significantly the proportion of the total noise contributed by either component. There was no significant change in the single channel conductance estimated from the noise spectra when pentobarbitone was co-applied with NMDA. The presence of two components in the noise spectra suggests that open channels may close to one of two closed states. Thus the noise spectra can be described by a model of the form:

$$\text{Closed} \underset{\alpha_1}{\overset{\beta_1}{\rightleftharpoons}} \text{open} \underset{\alpha_2}{\overset{\beta_2}{\rightleftharpoons}} \text{closed}$$

with α_1 and α_2 being the rate constants for channel closure and β_1 and β_2 the rate constants for channel opening. By adapting the solution for a simple sequential three state model proposed by Ruff (1977) to account for the effect of local anaesthetics on the noise evoked by acetylcholine at the end plate, it can be shown that the slow time constant τ_s is a meaure of mean cluster length (M_{cl}) and the fast time constant τ_f is approximated by the following relationship:

$$\tau_f \approx \frac{M_o \cdot M_g}{M_o + M_g}$$

where M_o is mean open time and M_g is mean gap length. The data derived from the noise analysis therefore suggest that mean cluster length is little affected by the anaesthetic but that the fall in current could be attributed to a fall in mean open time. Analysis of the single channel data from the cell attached patches supports this broad conclusion. Mean cluster length fell very little until the pentobarbitone concentration exceeded 200 μM while mean open time fell progressively with increasing anaesthetic concentration. The data from the outside-out patches were also consistent with this interpretation. The outside-out patches also clearly showed that pentobarbitone decreased the open probability of NMDA channels and that this reduction in P_o appeared to be of sufficient magnitude to account for the reduction in the

inward current evoked by NMDA. Thus the effects of pentobarbitone on the kinetics of the NMDA channels are similar whether they have been activated by low concentrations of agonist (single channel recording) or by high concentrations (noise analysis). Moreover, the data suggest that clusters represent the most stable form of gating.

What is the mechanism by which pentobarbitone blocks the channels? The answer to this question is complicated by the intricate gating exhibited by the NMDA channels. Using low concentrations of glutamate, Gibb & Colquhoun (1992) detected three open states and five closed states. In the data presented here with NMDA as the agonist, two open states and four closed states have been detected. These differences may simply reflect the different agonists used in each study. It is clear, therefore, that a definitive answer will not be easily attained. Nevertheless, by making some simplifying assumptions a partial account can be given. The key features of the single channel data may be summarised as follows: mean open time and mean burst length fall as the concentration of pentobarbitone increases, while mean gap time and mean cluster length are largely unchanged. If we neglect the fast openings on the grounds that they contribute little to the mean current, the simple three state model discussed earlier can be used to describe the channel gating and its modulation by pentobarbitone. The lifetime of any channel state equals the reciprocal of the sum of the rate constants leading away from that state. Since addition of anaesthetic shortens mean channel open time, the formation of an additional blocked state is likely. This additional state can be detected in the closed time distributions of the excised patches (see Figure 7) and in the increased area of the second component of the closed state distribution of the cell-attached patches (see Results). Moreover, the reciprocal of mean open time is a linear function of anaesthetic concentration as expected for an open state block (see Colquhoun & Hawkes, 1983). Burst length (and cluster length), however, also fall. So a simple sequential block model is not appropriate but an extended block model of the following type can provide a useful framework for describing the pentobarbitone-induced block of NMDA channels during steady-state activation:

$$\text{closed} \underset{\alpha_1}{\overset{\beta_1}{\rightleftharpoons}} \text{open} \underset{\alpha_2}{\overset{\beta_2}{\rightleftharpoons}} \text{closed}$$

$$b \downarrow\uparrow f[c]$$

$$\text{blocked} \underset{k_{-1}}{\overset{k_{+1}}{\rightleftharpoons}} (\text{closed} - \text{blocked})$$

This model, like the sequential open channel model of channel block can be used to make a number of quantitative predictions concerning the modulation of channel kinetics by anaesthetics (see Dilger *et al.*, 1992; Charlesworth & Richards, 1995). It predicts that mean open time (τ_{open}) will become shorter with increasing anaesthetic concentration according to the following relation:

$$\tau_{open} = \frac{1}{(\alpha_1 + \alpha_2) + f.[c]}$$

That this is the case is shown in Figure 6 from which we calculate the rate constant for channel block to be 1.03 μM^{-1} s^{-1} and $(\alpha_1 + \alpha_2) = 313$ s^{-1}. In agreement with the data, the model also predicts that mean gap time should not be concentration-dependent (this is true both for bursts and clusters – see Table 2). The model makes no explicit prediction about the effect of anaesthetics on mean length of bursts and clusters as the ratio of b/k_{+1} will determine the relative probability of transitions between the open blocked state and the closed block state. Although burst length declines with increasing concentration of anaesthetic, cluster length is less affected and this could be explained if $k_{-1} \approx \beta_1$ i.e. if the rate at which the closed blocked channel returns to the open block state is similar to the long time constant for channel opening.

Low concentrations of isoflurane have been shown to decrease the probability of channel opening without a significant effect on the mean open time of channels gated by NMDA but higher concentrations (> 1 mM) also reduce mean open time (Yang & Zorumski, 1991). Alkanols have similar effects (Weight *et al.*, 1991). Dissociative anaesthetics such as ketamine appear to block open NMDA channels preferentially and this block is both voltage-and use-dependent (Heutner & Bean, 1988; Macdonald *et al.*, 1987). In this case it is proposed that the channel closes while the anaesthetic is bound. Dissociation of the anaesthetic from the blocked state is very slow and the number of blocked channels accumulates as the preparation is repeatedly activated. Use-dependent local anaesthetic blockade of open voltage-gated sodium channels operates in a similar way (Butterworth & Strichartz, 1990). Marszalec & Narahashi (1993) have shown that pentobarbitone apparently induces a similar use-dependent block of kainate/AMPA channels.

To conclude, pentobarbitone does not significantly alter the balance between the various substates of the NMDA receptor. Rather, it appears that pentobarbitone inhibits the inward current resulting from application of NMDA by decreasing the mean open time of the channel so reducing the probability of the channel being in the open state during a burst. A differential effect of pentobarbitone on channel states is implied by the graded sensitivity of channel openings, bursts and clusters. Clusters appear to be the most stable form of gating.

We thank the Wellcome Trust for support and Dr Tony Horne for help in isolating neurones from the olfactory tubercle.

References

ASCHER, P., BREGESTOVSKI, P. & NOWAK, L. (1988). N-methyl-D-aspartate-activated channels of mouse central neurones in magnesium-free solutions. *J. Physiol.*, **399**, 207–226.

BUTTERWORTH, J.F. & STRICHARTZ, G.R. (1990). Molecular mechanism of local anesthesia: a review. *Anesthesiology*, **72**, 711–734.

CAI, Z. & MCCASLIN, P.P. (1993). Acute, chronic and differential effects of several anesthetic barbiturates on glutamate receptor activation in neuronal culture. *Brain Res.*, **611**, 181–186.

CHARLESWORTH, P., JACOBSON, I & RICHARDS, C.D. (1994). The action of pentobarbitone on the excitatory amino acid receptors dissociated from the rat olfactory brain. *J. Physiol.*, **475**, 153P.

CHARLESWORTH, P. & RICHARDS, C.D. (1995). Anaesthetic modulation of nicotinic ion channel kinetics in chromaffin cells. *Br. J. Pharmacol.*, **114**, 909–917.

CHIZHMAKOV, I.V., KISKIN, N.I. & KRISHTAL, O.A. (1992). Two types of steady-state desensitization of N-methyl-D-aspartate receptor in isolated hippocampal neurones of rat. *J. Physiol.*, **448**, 453–472.

COLQUHOUN, D. & HAWKES, A.G. (1983). The principles of stochastic interpretation of ion channel mechanisms. *In Single Channel Recording*. ed. Sackmann, B. & Neher, E. Ch 9, pp. 135–176. New York: Plenum.

CULL-CANDY, S.G., HOWE, J.R. & OGDEN, D.C. (1988). Noise and single channels activated by excitatory amino acids in rat cerebellar granule neurones. *J. Physiol.*, **400**, 189–222.

CULL-CANDY, S.G. & USOWICZ, M.M. (1989). On the multiple-conductance single channels activated by excitatory amino acids in large cerebellar neurones of the rat. *J. Physiol.*, **415**, 555–582.

CLAPHAM, D.E. & NEHER, E. (1984). Substance P reduces acetylcholine-induced currents in isolated bovine chromaffin cells. *J. Physiol.*, **347**, 255–277.

CRAWFORD, J.M. & CURTIS, D.R. (1966). Pharmacological studies on feline Betz cells. *J. Physiol.*, **186**, 121–138.

DILGER, J.P., BRETT, R.S. & LESKO, L.A. (1992). Effects of isoflurane on acetylcholine receptor channels. 1. Single-channel currents. *Molec. Pharmacol.*, **41**, 127–133.

GASIC, G.P. & HEINEMANN, S. (1991). Receptors coupled to ionic channels: the glutamate receptor family. *Curr. Op. Neurobiol.*, **1**, 20–26.

GIBB, A.J. & COLQUHOUN, D. (1992). Activation of N-methyl-D-aspartate receptors by L-glutamate in cells dissociated from adult rat hippocampus. *J. Physiol.*, **456**, 143–179.

HAMILL, O.P., MARTY, A., NEHER, E., SACKMANN, B & SIGWORTH, F.J. (1981). Improved patchclamp techniques for high resolution current recordings from cells and cell-free membrane patches. *Pflugers Archiv.*, **391**, 85–100.

HEADLEY, P.M. & GRILLNER, S. (1990). Excitatory amino acids and synaptic transmission: the evidence for a physiological function. *Trends Pharmacol. Sci.*, **11**, 205–211.

HEUTNER, J.E. & BEAN, B.P. (1988). Block of N-methyl-D-aspartate activated current by the anticonvulsant MK-801: selective binding to open channels. *Proc. Natl. Acad. Sci. U.S.A.*, **85**, 1307–1311.

JACOBSON, I., BUTCHER, S & HAMBERGER, A. (1986). An analysis of the effects of excitatory amino acid receptor antagonists on evoked field potentials in the olfactory bulb. *Neuroscience*, **19**, 267–273.

JACOBSON, I. & HAMBERGER, A. (1986). Effects of kynurenic acid on evoked extracellular field potentials in the rat olfactory bulb *in vivo*. *Brain Res.*, **386**, 389–392.

JACOBSON, I. & LI, X. (1992). Whole cell currents activated by N-methyl-D-aspartate in freshly isolated neurones from the olfactory bulb of the rat. *Neurosci. Res. Commun.*, **10**, 177–185.

KAY, A.R. & WONG, R.K.S. (1986). Isolation of neurons suitable for patch-clamping from adult mammalian central nervous systems. *J. Neurosci. Meth.*, **6**, 227–238.

KRISHTAL, O.A. & PIDOPLICHKO, V.I. (1980). A receptor for protons in the nerve cell membrane. *Neuroscience*, **5**, 2325–2327.

KUTSUWADA, T., KASHIWABUCHI, N., MORI, H., SAKIMURA, K., KUSHIYA, E., ARAKI, K., MASAKI, H., KUMANISHI, T., ARAKAWA, M. & MISHINA, M. (1992). Molecular diversity of the NMDA receptor channel. *Nature*, **358**, 36–41.

MACDONALD, J.F., MILJKOVIC, Z. & PENNEFATHER, P. (1987). Use-dependent block of excitatory amino acid currents in cultured neurons by ketamine. *J. Neurophysiol.*, **58**, 251–266.

MARSZALEC, W. & NARAHASHI, T. (1993). Use-dependent pentobarbital block of kainate and quisqualate currents. *Brain Res.*, **608**, 7–15.

MILJKOVIC, Z & MACDONALD, J.F. (1986). Voltage-dependent block of excitatory amino acid currents by pentobarbital. *Brain Res.*, **376**, 396–399.

MONYER, H., SPRENGEL, R., SCHOEPFER, R., HERB, A., HIGUCHI, M., LOMELI, H., SAKMANN, B. & SEEBURG, P.H. (1992). Heteromeric NMDA receptors: molecular and functional distinction of subtypes. *Science*, **256**, 1217–1221.

PATLAK, J.B. (1988). Sodium channel subconductance levels measured with a new variance-mean analysis. *J. Gen. Physiol.*, **92**, 413–430.

RICHARDS, C.D. (1972). On the mechanism of barbiturate anaesthesia. *J. Physiol.*, **227**, 749–767.

RICHARDS, C.D., RUSSELL, W.J. & SMAJE, J.C. (1975). The action of ether and methoxyflurane on synaptic transmission in isolated preparations of the mammalian cortex. *J. Physiol.*, **248**, 121–142.

RICHARDS, C.D. & SMAJE, J.C. (1976). Anaesthetics depress the sensitivity of cortical neurones to L-glutamate. *Br. J. Pharmacol.*, **58**, 347–357.

RUFF, R.L. (1977). A quantitative analysis of local anaesthetic alteration of miniature end-plate currents and end-plate current fluctuations. *J. Physiol.*, **264**, 89–124.

SACHS, F., NEIL, J. & BARKAKATI, N. (1982). The automated analysis of data from single ion channels. *Pflügers Archiv.*, **395**, 331–340.

SANDBERG, M., BRADFORD, H.F. & RICHARDS, C.D. (1984). Effect of lesions of the olfactory bulb on the levels of amino acids and related enzymes in the olfactory cortex of the guinea pig. *J. Neurochem.*, **43**, 276–279.

SAWADA, S. & YAMAMOTO, C. (1985). Blocking action of pentobarbital on receptors for excitatory amino acids in the guinea-pig hippocampus. *Exp. Brain Res.*, **59**, 226–231.

WATKINS, J.C., KROGSGAARD-LARSEN, P. & HONORE, T. (1990). Structure-activity relationships in the development of excitatory amino acid receptor agonists and competitive antagonists. *Trends Pharmacol.*, **11**, 25–33.

WEIGHT, F.F., LOVINGER, D.M., WHITE, G. & PEOPLES, R.W. (1991). Alcohol and anesthetic actions on excitatory amino acid-activated ion channels. *Ann. NY Acad. Sci.*, **625**, 97–107.

WILLIAMS, K., RUSSELL, S.L., SHEN, Y.M., & MOLINOFF, P.B. (1993). Developmental switch in the expression of NMDA receptors occurs *in vivo* and *in vitro*. *Neuron*, **10**, 267–278.

YANG, J. & ZORUMSKI, C.F. (1991). Effects of isoflurane on N-methyl-D-aspartate gated ion channels in cultured rat hippocampal neurons. *Ann. NY Acad. Sci.*, **625**, 287–289.

(Received May 5, 1995
Revised July 25, 1995
Accepted August 14, 1995)